Copyright ⓒ 2012 KSII

Performance Analysis And Optimization For AF Two-Way Relaying With Relay Selection Over Mixed Rician And Rayleigh Fading

Zhangjun Fan[1], Daoxing Guo[1] , Bangning Zhang[1] and Li Zeng[2]
[1] Institute of Communications Engineering, PLA University of Science and Technology
Nanjing, Jiangsu 210007 - China
[2] Institute of Command Automation, PLA University of Science and Technology
Nanjing, Jiangsu 200433 - China
[e-mail: fzjicepangpang@126.com, {DX_guo, zhangbn}@163.com, mofistova@qq.com]
*Corresponding author: Zhangjun Fan

Received September 16, 2012; revised November 18, 2012; accepted December 12, 2012; published December 27, 2012

Abstract

In this paper, we analyze the performance of an amplify-and-forward (AF) two-way relaying system, where two sources exchange information via the aid of an intermediate relay that is selected among multiple relays according to max-min criterion. We consider a practical scenario, where one source-relay link undergoes Rician fading, and the other source-relay link is subject to Rayleigh fading. To be specific, we derive a tight lower bound for the outage probability. From this lower bound, the asymptotic outage probability and average symbol error rate (SER) expressions are derived to gain insight into the system performance at high signal-to-noise ratio (SNR) region. Furthermore, we investigate the optimal power allocation (PA) with fixed relay location (RL), optimal RL with fixed PA and joint optimization of PA and RL to minimize the outage probability and average SER. The analytical expressions are verified through Monte Carlo simulations, where the positive impact of Rician factor on the system performance is also illustrated. Simulation results also validate the effectiveness of the proposed PA and relay positioning schemes.

Keywords: Two-way relaying, outage probability, average symbol error rate, power allocation, relay location

http://dx.doi.org/10.3837/tiis.2012.12.014

1. Introduction

Nowadays, two-way relaying has attracted wide research interest, due to its ability to improve spectral efficiency [1]. In a two-way relaying system (TWRS), two sources exchange information during two time slots via the aid of an intermediate relay [1]. Two sources transmit simultaneously to a relay during the first time slot, and the relay broadcasts the received signals after some processing during the second time slot. In general, the traditional decode-and-forward (DF) protocol and amplify-and-forward (AF) protocol used in one-way relaying system (OWRS) can be applied to TWRS [1]. In the DF scheme, the relay decodes the signals received, manipulates XOR operation in bit-level and broadcasts to both sources [2]. In the AF scheme, the relay simply amplifies the signals received and broadcasts the amplified signals to both sources [3]. AF protocol thus has lower implementation complexity than DF protocol; therefore we focus on AF protocol in this paper.

It has been shown that the performance of TWRS can be improved by employing multiple relays to assist transmission. The authors in [4] have proposed a distributed space-time coding scheme for the AF TWRS, which can achieve full diversity order if the number of symbols in a frame is no less than the number of relays. Nevertheless, the distributed space-time coding requires significant amounts of coordination for both signaling and synchronization, which increases the implementation complexity. Relay selection (RS) has been shown to be an attractive alternative to combat this drawback [5], and many works have contributed to the performance analysis of AF TWRS with RS [6][7][8][9][10][11]. The authors in [6] have proposed a RS criterion for AF TWRS, with aim to maximize the overall channel capacity. In addition, performance bounds on average sum-rate, average symbol error rate (SER) and outage probability were provided in [6]. Another RS criterion, termed as max-min RS, has been proposed in [7]. The average SER of max-min RS was analyzed in [8] for binary phase shift keying (BPSK) over Rayleigh fading channels. The authors in [9] have analyzed the outage probability, average sum-rate for max-min RS over Nakagami-m fading channels. Taking into account channel estimation error, the outage probability and average bit error rate of max-min RS have been investigated in [10]. Furthermore, the authors in [11] have analyzed the diversity orders of various RS schemes, including best-relay selection, best-worse-channel selection and maximum-harmonic-mean selection. However, all the above mentioned works did not consider mixed Rician and Rayleigh fading channels. It is well known that it would be more appropriate to model one source to relay link as Rician fading in cellular networks, due to strong line-of-sight (LOS) component [12]. This is the motivation for our investigation of the performance of AF TWRS with relay selection over mixed Rician and Rayleigh fading channels. It is worthy noting that the performance of OWRS over mixed Rician and Rayleigh fading has been investigated in [13][14]. Nevertheless, the analysis method for OWRS cannot be applied to TWRS directly because of the presence of bidirectional transmission flows in TWRS.

Another line of research has been focused on power allocation (PA) and relay positioning (RP) for TWRS [8][15][16][17][18]. A closed-form PA solution has been provided based on the asymptotic average SER expression [8]. Besides, optimum PA schemes based on instantaneous channel state information have been proposed in [15][16][17]. The authors in [16] have also proposed a sub-optimum PA algorithm, aiming to minimize the asymptotic outage probability of AF TWRS with max-min RS over Nakagami-m fading channels.

Another way to improve the system performance is to perform relay location (RL) optimization or joint PA and RL optimization. For TWRS, the optimal RL has been derived to minimize the outage probability and energy consumption in [17] and [18], respectively. To the best of the authors' knowledge, the joint PA and RL optimization for TWRS has not yet been found in open literatures. However, a number of works such as [19][20][21][22][23] have addressed the joint optimization problem of PA and RL for OWRS over various scenarios.

In light of aforementioned researches, in this paper we analyze the performance of AF TWRS with max-min relay selection[1]. Specially, we consider the mixed Rician and Rayleigh fading channels, which would be more appropriate to model the practical channels in cellular networks [12][13]. First, we derive a tight lower bound for the outage probability. To obtain more insights into the system performance at high signal-to-noise ratio (SNR), we also derive the asymptotic outage probability and average SER expressions, from which the diversity order is revealed. Furthermore, we optimize the outage probability and average SER by proposing PA scheme with fixed RL and RP scheme with fixed PA, which are derived from the asymptotic expressions. An iterative joint PA and RL optimization algorithm is also proposed to further minimize the outage probability and average SER. Finally, extensive Monte Carlo simulations are conducted to verify the analytical expressions. The effectiveness of proposed PA and RP schemes are also validated by simulation results.

The rest of this paper is organized as follows. Section 2 describes the system model, and section 3 presents the analysis of outage probability and average SER. In section 4, the proposed PA and RP schemes are presented. Simulation results and discussions are provided in section 5. We draw the conclusions in section 6.

Notation: Throughout this paper, the operators $E[\bullet]$ and $\Pr[\bullet]$ represent expectation and probability, respectively. $f_x(\bullet)$ and $F_x(\bullet)$ denote the probability density function (PDF) and cumulative distribution function (CDF) of a random variable x, respectively. $o(\bullet)$ denotes the high-order infinitesimal.

2. System Model

Consider an AF TWRS consisting of two sources (denoted as T_a and T_b), which wish to exchange information with the help of N relays (denoted as $R_1, R_2, \cdots R_N$), as shown in **Fig. 1**. There is no direct link between T_a and T_b due to high shadowing, and all links between sources and relays are independent. All nodes in the system operate in half-duplex mode, and time-division duplex (TDD) is adopted. The channels are assumed to undergo block, quasi-static flat fading, namely they keep constant within one round of information exchange and change independently from one round to another round. The channel from T_a to R_j is denoted by $h_{a,j}$, and is subject to Rician fading owing to one strong LOS component, $j = 1, 2, \cdots, N$. The channel from T_b to R_j is denoted by $h_{b,j}$, and undergoes Rayleigh

[1] The differences between the performance analysis of this paper and those in [8][9] mainly consist of two aspects: (i) we consider the mixed Rician and Rayleigh fading channels, while [8] and [9] considered the Rayleigh and Nakagami-m fading channels, respectively; (ii) Unlike the works in [8][9], we assume both sources having not necessarily identical transmitting power, which matches the practical scenarios more appropriately.

fading[2]. Since the system works in TDD mode and the channels are block quasi-static fading, the channels are reciprocal, i.e., the channel from R_j to T_k is also described by $h_{k,j}, k=a,b$, $j=1,2,\cdots,N$. Let $d_{k,j}$ denote the distance between T_k and $R_j, k=a,b, j=1,2,\cdots N$. We assume, as in [6][9], the relays are cluster located, and thus the inter-relay distances are small enough compared with $d_{k,j}$. So, we reasonably assume $d_{k,j}=d_k, k=a,b, j=1,2,\cdots N$. As such, links $T_k \leftrightarrow R_i$ and $T_k \leftrightarrow R_j$ have the same average fading power, which is denoted by $\Omega_k = d_k^{-v}$ with v as a path loss exponent, $k=a,b,\forall i, j=1\cdots N$. Accordingly, the PDF of $|h_{a,j}|^2$ is given by $f_{|h_{a,j}|^2}(x)=\frac{(1+J)e^{-J}}{\Omega_a}e^{-\frac{(1+J)x}{\Omega_a}} I_0\left(2\sqrt{\frac{J(1+J)x}{\Omega_a}}\right)$ ([24], Eq. (2.16)), where $J>0$ denotes the Rician factor, and $I_0(\bullet)$ denotes the zeroth-order modified Bessel function of the first kind ([25], Eq. (8.431.1)). The PDF of $|h_{b,j}|^2$ is given by $f_{|h_{b,j}|^2}(y)=e^{-y/\Omega_b}/\Omega_b$.

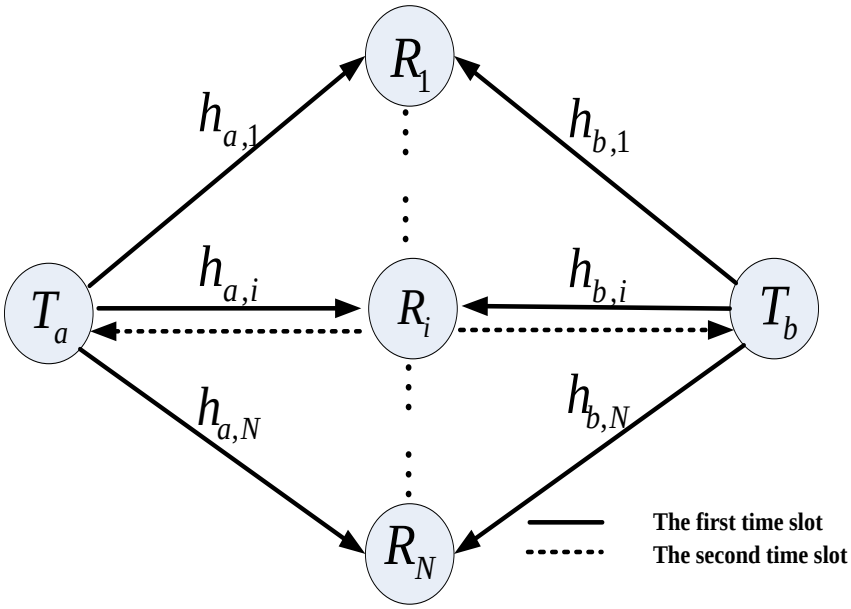

Fig. 1 Block diagram of AF TWRS with RS.

One round of information exchange between T_a and T_b consists of two time slots. In the first time slot, T_a and T_b transmit simultaneously to all relays. The signal received at R_j $(1 \le j \le N)$ can be written by

$$y_j = \sqrt{p_a}h_{a,j}x_a + \sqrt{p_b}h_{b,j}x_b + n_j \tag{1}$$

where p_k and x_k denote the transmitting power and transmitted signal with average unit

[2] This assumption is valid in practice. For example, in relay enhanced cellular networks, the base station and relays are located in an environment where a LOS exists. Therefore, the base station to relays links can be modeled as Rician fading. Meanwhile, the mobile user is usually surrounded by multiple scatters, and thus the relays to mobile user links only experience Rayleigh fading [13].

energy of T_k, $k=a,b$, respectively, n_j denotes the additive white Gaussian noise (AWGN) with zero mean and unit variance at R_j. In the second time slot, only the best relay is selected to transmit to both sources after amplifying the signal it has received. In this paper, we adopt the max-min RS scheme, namely the best relay R_i is selected according to $i=\arg\max_{j=1,2\cdots N}\min\left(\gamma_{a,j},\gamma_{b,j}\right)$ [8][9], where $\gamma_{a,j}$ and $\gamma_{b,j}$ denote the instantaneous SNRs received at T_a and T_b, respectively, when R_j is selected to help transmission. Supposing R_i is selected, the signals received at T_a and T_b can be respectively written as

$$y_a=\sqrt{p_a p_r}Gh_{a,i}^2x_a+\sqrt{p_b p_r}Gh_{a,i}h_{b,i}x_b+\sqrt{p_r}Gh_{a,i}n_i+n_a \tag{2}$$

$$y_b=\sqrt{p_a p_r}Gh_{a,i}h_{b,i}x_a+\sqrt{p_b p_r}Gh_{b,i}^2x_b+\sqrt{p_r}Gh_{b,i}n_i+n_b \tag{3}$$

where p_r denotes the transmitting power of relay R_i, $G=\sqrt{1\Big/\left(p_a\left|h_{a,i}\right|^2+p_b\left|h_{b,i}\right|^2+1\right)}$ is the amplifying factor, n_k denotes the AWGN with zero mean and unit variance at T_k, $k=a,b$. After self-information cancelation and some elementary manipulations, the instantaneous SNRs at T_a and T_b can be respectively represented by

$$\gamma_{a,i}=\frac{p_b p_r\left|h_{a,i}\right|^2\left|h_{b,i}\right|^2}{\left(p_a+p_r\right)\left|h_{a,i}\right|^2+p_b\left|h_{b,i}\right|^2+1} \tag{4}$$

$$\gamma_{b,i}=\frac{p_a p_r\left|h_{a,i}\right|^2\left|h_{b,i}\right|^2}{p_a\left|h_{a,i}\right|^2+\left(p_b+p_r\right)\left|h_{b,i}\right|^2+1} \tag{5}$$

3. Performance Analysis

In this section, we derive important performance measures for the AF TWRS with max-min RS, including outage probability, average SER and diversity order.

3.1 Outage Probability

In a TWRS, an outage event occurs when any end-to-end transmission is in outage, i.e., when either $\gamma_{a,i}$ or $\gamma_{b,i}$ falls below a predefined threshold γ_{th}. Therefore, the definition of outage probability is given by [9]

$$P_{out}=\Pr\left[\max_{j=1,2\cdots N}\min\left(\gamma_{a,j},\gamma_{b,j}\right)<\gamma_{th}\right] \tag{6}$$

Since it is mathematically intractable to derive the closed-form exact outage probability expression, we present a closed-form lower bound for the outage probability in the following proposition.

Proposition 1: The outage probability of the AF TWRS with max-min RS can be lower bounded by

$$P_{out}^{l}=\begin{cases}\left[1-Q\left(\sqrt{2J},\sqrt{\dfrac{2\lambda(1+J)\gamma_{th}}{p_r}}\right)e^{-\frac{\theta\eta_2\gamma_{th}}{p_r}}\right]^N & 1\le\eta_1\\ \left[1-Q\left(\sqrt{2J},\sqrt{\dfrac{2\lambda(1+J)\gamma_{th}}{\eta_1 p_r}}\right)e^{-\frac{\theta\gamma_{th}}{p_r}}\right]^N & \eta_2\le 1\\ \left[1-Q\left(\sqrt{2J},\sqrt{\dfrac{2\lambda(1+J)\gamma_{th}}{\eta_1 p_r}}\right)e^{-\frac{\theta\eta_2\gamma_{th}}{p_r}}\right]^N & \eta_1<1<\eta_2\end{cases} \tag{7}$$

where $Q(\bullet,\bullet)$ is the first-order Marcum Q function ([24], Eq. (4.32)), $\lambda=1/\Omega_a$, $\theta=1/\Omega_b$, $\eta_1=p_a/(p_b+p_r)$ and $\eta_2=(p_a+p_r)/p_b$.

Proof: We first derive

$$P_{min}=\Pr\left[\min(\gamma_{a,j},\gamma_{b,j})<\gamma_{th}\right]=\Pr\left[\gamma_{a,j}<\gamma_{th},\gamma_{a,j}<\gamma_{b,j}\right]+\Pr\left[\gamma_{b,j}<\gamma_{th},\gamma_{b,j}<\gamma_{a,j}\right] \tag{8}$$

According to the results in [26], $\gamma_{a,j}$ and $\gamma_{b,j}$ can be tightly upper bounded by

$$\begin{aligned}\gamma_{a,j}&<\frac{p_b p_r|h_{a,j}|^2|h_{b,j}|^2}{(p_a+p_r)|h_{a,j}|^2+p_b|h_{b,j}|^2}\\ \gamma_{b,j}&<\frac{p_a p_r|h_{a,j}|^2|h_{b,j}|^2}{p_a|h_{a,j}|^2+(p_b+p_r)|h_{b,j}|^2}.\end{aligned} \tag{9}$$

Substituting (9) into (8) and processing some elementary manipulations, yields

$$\begin{aligned}&P_{\min}=\Pr\left[\min(\gamma_{a,j},\gamma_{b,j})<\gamma_{th}\right]\\ &>\Pr\left[\gamma_{a,j}<\gamma_{th},(\eta_2-1)|h_{a,j}|^2>(1/\eta_1-1)|h_{b,j}|^2\right]+\Pr\left[\gamma_{b,j}<\gamma_{th},(\eta_2-1)|h_{a,j}|^2<(1/\eta_1-1)|h_{b,j}|^2\right]\end{aligned} \tag{10}$$

We consider three cases to solve (10) in the following.

Case 1 ($1\le\eta_1$): Since $\Pr\left[(\eta_2-1)|h_{a,j}|^2>(1/\eta_1-1)|h_{b,j}|^2\right]=1$ and the second term on the right of (10) equals to zero, we have $P_{\min}=\Pr\left[\gamma_{a,j}<\gamma_{th}\right]$ in this case. By using the inequality $xy/(x+y)\le\min(x,y)$ [27], we obtain the lower bound of P_{min} as

$$\begin{aligned}P_{\min}&=1-\Pr\left[\gamma_{a,j}\ge\gamma_{th}\right]\ge 1-\Pr\left[\min\left(p_r|h_{a,j}|^2,p_r|h_{b,j}|^2/\eta_2\right)\ge\gamma_{th}\right]\\ &=1-\Pr\left[|h_{a,j}|^2\ge\gamma_{th}/p_r\right]\Pr\left[|h_{b,j}|^2\ge\eta_2\gamma_{th}/p_r\right] \qquad (a)\\ &=1-Q\left(\sqrt{2J},\sqrt{2\lambda(1+J)\gamma_{th}/p_r}\right)e^{-\theta\eta_2\gamma_{th}/p_r} \qquad (b)\end{aligned} \tag{11}$$

Step (a) holds because $|h_{a,j}|^2$ and $|h_{b,j}|^2$ are independent. Step (b) results from ([28], Eq. (8))

$$\int_x^\infty\lambda(1+J)e^{-J}e^{-\lambda(1+J)t}I_0\left(2\sqrt{\lambda J(1+J)t}\right)dt=Q\left(\sqrt{2J},\sqrt{2\lambda(1+J)x}\right) \tag{12}$$

Case 2 ***($\eta_2 \le 1$)***: In this case, we have $P_{\min} = \Pr\left[\gamma_{b,j} < \gamma_{th}\right]$. Following the similar steps taken in ***Case 1***, we get the lower bound of P_{min} as

$$P_{\min} \ge 1 - Q\left(\sqrt{2J}, \sqrt{\frac{2\lambda(1+J)\gamma_{th}}{\eta_1 p_r}}\right) e^{-\frac{\theta\gamma_{th}}{p_r}} \tag{13}$$

Case 3 ***($\eta_1 < 1 < \eta_2$)***: The derivation of $P_{\min}$ in this case is different from those in ***Case 1*** and ***Case 2***. From the definition of $P_{\min}$, we have

$$\begin{aligned}
P_{\min} &= \Pr\left[\min\left(\gamma_{a,j}, \gamma_{b,j}\right) < \gamma_{th}\right] = 1 - \Pr\left[\min\left(\gamma_{a,j}, \gamma_{b,j}\right) \ge \gamma_{th}\right] \\
&\ge 1 - \Pr\left[\min\left(p_r |h_{a,j}|^2, p_r |h_{b,j}|^2 / \eta_2, \eta_1 p_r |h_{a,j}|^2, p_r |h_{b,j}|^2\right) \ge \gamma_{th}\right] \quad (a) \\
&= 1 - \Pr\left[\min\left(\eta_1 p_r |h_{a,j}|^2, p_r |h_{b,j}|^2 / \eta_2\right) \ge \gamma_{th}\right] \quad (b) \quad (14) \\
&= 1 - \Pr\left[\eta_1 p_r |h_{a,j}|^2 \ge \gamma_{th}\right] \Pr\left[p_r |h_{b,j}|^2 / \eta_2 \ge \gamma_{th}\right] \quad (c) \\
&= 1 - Q\left(\sqrt{2J}, \sqrt{2\lambda(1+J)\gamma_{th}/\eta_1 p_r}\right) e^{-\theta\eta_2\gamma_{th}/p_r} \quad (d)
\end{aligned}$$

Step (a) results from the inequality $xy/(x+y) \le \min(x,y)$ [27], step (b) holds for the constraint $\eta_1 < 1 < \eta_2$, step (c) holds for the independence of $|h_{a,j}|^2$ and $|h_{b,j}|^2$, and step (d) derives from (12).

Now, we have obtained the expression of P_{min}. By using the order statistics [29], we get the desired result from (6), as presented in (7).■

Simulation results later will show that the lower bound in (7) is close to the simulated outage probability from medium to high SNR regime. Since the system will not work at low SNR region in practice, the lower bound (7) acts as guideline for system design. To obtain better insight into the system's outage behavior at high SNR, we present the asymptotic outage probability expression in the following proposition.

Proposition 2: The asymptotic outage probability at high SNR for the AF TWRS with max-min RS is given by

$$P_{out}^{a} = (c\gamma_{th})^{N} \tag{15}$$

$$c = \begin{cases} \dfrac{\lambda(1+J)e^{-J}}{p_r} + \dfrac{\theta\eta_2}{p_r} & 1 \le \eta_1 \\ \dfrac{\lambda(1+J)e^{-J}}{\eta_1 p_r} + \dfrac{\theta}{p_r} & \eta_2 \le 1 \\ \dfrac{\lambda(1+J)e^{-J}}{\eta_1 p_r} + \dfrac{\theta\eta_2}{p_r} & \eta_1 < 1 < \eta_2 \end{cases} \tag{16}$$

Proof: Let

$$x = \begin{cases} \gamma_{th}/p_r & 1 \le \eta_1 \\ \gamma_{th}/(\eta_1 p_r) & 1 > \eta_1 \end{cases} \quad y = \begin{cases} \gamma_{th}/p_r & 1 \ge \eta_2 \\ \eta_2\gamma_{th}/p_r & 1 < \eta_2 \end{cases} \tag{17}$$

As the transmitting power approaches infinity, x and y approach zeros. After substituting the infinite-series representation of $I_0(\bullet)$ into (12) ([25], Eq. (8.447.1)), using Taylor series expansion, and processing some algebraic manipulations, the first-order expansion of $Q\left(\sqrt{2J},\sqrt{2\lambda(1+J)x}\right)$ can be written by

$$Q\left(\sqrt{2J},\sqrt{2\lambda(1+J)x}\right)=1-\lambda(1+J)e^{-J}x+o(x) \tag{18}$$

Substituting (18) and $e^{-\theta y}=1-\theta y+o(y)$ into (7), neglecting the high-order infinitesimal terms, yields the asymptotic outage probability expression, as presented in (15) and (16).■

As will be shown in section 5, (15) excellently approximates the simulated outage probability at high SNR. (15) and (16) reveal that the AF TWRS with max-min RS can achieve a diversity order of N, which demonstrates the benefits of employing multiple relays to assist transmission.

3.2 Average Symbol Error Rate

Define $P_{e,a}$ and $P_{e,b}$ as the average SER at T_a and T_b, respectively. For a TWRS, $P_e=\max\left(P_{e,a},P_{e,b}\right)$, which reflects the average SER of the worse direction, can be employed to quantify the system's transmission reliability [10]. Since it is cumbersome to derive the exact expression of P_e, in this subsection we derive an asymptotic expression of P_e at high SNR to examine the system's SER performance.

The instantaneous SER of coherent modulation is in the form $P_s(\gamma)=aQ\left(\sqrt{b\gamma}\right)$ [24], where γ is the instantaneously received SNR, $Q(x)=\frac{1}{\sqrt{2\pi}}\int_x^\infty e^{-t^2/2}dt$ is Gaussian-Q function, a and b are modulation type dependent constants. Specially, $a=4\left(1-1/\sqrt{M}\right)$, $b=3/(M-1)$ for M-ary quadrature amplitude modulation and $a=2$, $b=\sin^2\pi/M$ for M-ary phase-shift keying ($M\geq 4$). According to the result in [30], the average SER P_e can be calculated by

$$P_e=\frac{a\sqrt{b}}{2\sqrt{\pi}}\int_0^\infty\frac{e^{-bx}}{\sqrt{x}}F_{\gamma_{\min}}(x)dx \tag{19}$$

where $\gamma_{\min}=\max\limits_{j=1,2\cdots N}\min\left(\gamma_{a,j},\gamma_{b,j}\right)$. From the derivation of asymptotic outage probability (15), we can approximate $F_{\gamma_{\min}}(x)$ at high SNR as

$$F_{\gamma_{\min}}(x)=(cx)^N \tag{20}$$

By substituting (20) into (19) and solving resultant integral with the help of ([25], Eq. (3.381.4)), we obtain the asymptotic average SER expression P_e as

$$P_e=\frac{ac^N\sqrt{b}}{2\sqrt{\pi}}\frac{\Gamma(N+0.5)}{b^{N+0.5}} \tag{21}$$

where $\Gamma(s)=\int_0^\infty t^{s-1}e^{-t}dt$ is Gamma function ([25], Eq. (8.310.1)).

As can be seen in section 5, (21) approximates the average SER quite well at high SNR. (16) and (21) also illustrates the positive impact of Rician factor on the average SER

performance compared to Rayleigh fading, which can be explained as follows: since e^J can be expanded as $\sum_{i=0}^{\infty} J^i/i!$, we have $e^J > 1+J$ for $J>0$, which means that $(1+J)e^{-J}<1$. In other words, we have the strict inequality $\lambda(1+J)e^{-J}<\lambda$ for $J>0$.

4. Performance Optimization

In this section, we first optimize the PA to minimize the outage probability and average SER, with the total transmitting power and RL fixed. Then, the optimal RL solution with fixed PA is derived to improve the system performance. Thereafter, an iterative algorithm is proposed to jointly optimize the PA and RL.

4.1 Optimizing Power Allocation under Fixed Relay Location

Supposing the RL (d_a and d_b) and total transmitting power $p = p_a + p_b + p_r$ are fixed, the outage probability and average SER can be simultaneously minimized by solving the following optimization problem:

$$\begin{aligned} &(p_a, p_b, p_r) = \arg \min_{p_a, p_b, p_r} c \\ &s.t. \quad p_a + p_b + p_r = p, \\ &\quad p_a > 0, p_b > 0, p_r > 0 \end{aligned} \tag{22}$$

We consider three cases to solve (22). For notation simplicity, we denote $\lambda(1+J)e^{-J}$ as ω in the following.

Case A ($1 \le \eta_1$)***:*** In this case, (22) can be transformed to

$$\begin{aligned} &(p_a, p_b, p_r) = \arg \min_{p_a, p_b, p_r} \frac{\omega}{p_r} + \frac{\theta(p-p_b)}{p_b p_r} \\ &s.t. \quad p_a + p_b + p_r = p \\ &\quad p_b + p_r \le p_a \\ &\quad p_a > 0, p_b > 0, p_r > 0 \end{aligned} \tag{23}$$

It is observed from (23) that the objective function decreases with p_b increasing. Therefore, the optimum value is attained when $p_b + p_r = p_a$. After substituting $p_b + p_r = p_a$ into $p_a + p_b + p_r = p$, we obtain the optimum transmitting power of T_a as $p_a = 0.5p$. Substituting $p_b = 0.5p - p_r$ into the objective function, yields

$$\frac{\omega}{p_r} + \frac{\theta(0.5p + p_r)}{(0.5p - p_r)p_r} \tag{24}$$

The second-order derivative of (24) with respect to p_r is in the following form:

$$\frac{2\omega}{p_r^3} + \frac{0.25\theta\left[8p_r^3 + 3pp_r^2 + (3p_r - p)^2\right]}{(0.5p - p_r)^3 p_r^3} \tag{25}$$

It is easily verified that (25) is positive in the interval $p_r \in (0, 0.5p)$, which implies that (24) is a strictly convex function of p_r for $p_r \in (0, 0.5p)$. Thus, we could obtain the optimum p_r by setting the first-order derivative of (24) to zero. After differentiating (24) with respect

to p_r, and setting the resultant differential to zero, we obtain the following equation:

$$(\theta-\omega)p_r^2+(\omega+\theta)pp_r-0.25(\omega+\theta)p^2=0 \tag{26}$$

After some algebraic manipulations on (26), the optimum transmitting power of relay is obtained as

$$p_r=\begin{cases}\dfrac{\left[-(\omega+\theta)+\sqrt{2\theta^2+2\omega\theta}\right]p}{2(\theta-\omega)} & \omega\neq\theta\\ 0.25p & \omega=\theta\end{cases} \tag{27}$$

Note that we have omitted the other solution to (26) when $\omega\neq\theta$, since it is larger than $0.5p$. With $p_b+p_r=0.5p$, the optimum transmitting power of T_b is given by

$$p_b=\begin{cases}\dfrac{\left[2\theta-\sqrt{2\theta^2+2\omega\theta}\right]p}{2(\theta-\omega)} & \omega\neq\theta\\ 0.25p & \omega=\theta\end{cases} \tag{28}$$

Case B ***(*** $1\geq\eta_2$ ***)***: Following the similar steps taken in ***Case A***, we obtain the optimum power allocation as

$$p_a=\begin{cases}\dfrac{\left[2\omega-\sqrt{2\omega^2+2\omega\theta}\right]p}{2(\omega-\theta)} & \omega\neq\theta\\ 0.25p & \omega=\theta\end{cases} \tag{29}$$

$$p_r=\begin{cases}\dfrac{\left[-(\omega+\theta)+\sqrt{2\omega^2+2\omega\theta}\right]p}{2(\omega-\theta)} & \omega\neq\theta\\ 0.25p & \omega=\theta\end{cases} \tag{30}$$

$$p_b=0.5p \tag{31}$$

Case C ***(*** $\eta_1<1<\eta_2$ ***)***: In this case, the optimization problem (22) is equivalent to

$$\begin{aligned}&(p_a,p_b,p_r)=\arg\min_{p_a,p_b,p_r}\frac{\omega(p_b+p_r)}{p_ap_r}+\frac{\theta(p_a+p_r)}{p_bp_r}\\ &s.t.\quad p_a+p_b+p_r=p\\ &\quad\ p_a-p_b-p_r<0\\ &\quad\ p_b-p_a-p_r<0\\ &\quad\ p_a>0,p_b>0,p_r>0\end{aligned} \tag{32}$$

To simplify the derivation, we first ignore the inequality constraints in (32), and focus on solving the following optimization problem:

$$\begin{aligned}&(p_a,p_b,p_r)=\arg\min_{p_a,p_b,p_r}\frac{\omega(p_b+p_r)}{p_ap_r}+\frac{\theta(p_a+p_r)}{p_bp_r}\\ &s.t.\quad p_a+p_b+p_r=p\end{aligned} \tag{33}$$

Since the objective function and constraint function of (33) are differentiable, we solve the Karush-Kuhn-Tucker (KKT) equations to find the optimal value of (33)(the KKT condition is the necessary condition even for nonconvex problem, i.e., the optimal solution of an

optimization problem must satisfy the KKT conditions [31][32]). Therefore, we can construct a Lagrangian function L from (33) as

$$L=\frac{\omega p}{p_a p_r}+\frac{\theta p}{p_b p_r}-\frac{\omega+\theta}{p_r}+\tau\left(p_a+p_b+p_r-p\right) \tag{34}$$

where τ is the Lagrangian multiplier. Setting the first-order derivatives of L with respect to p_a, p_b, p_r and τ to zero, yields the following KKT equations:

$$\begin{gathered}\frac{-\omega p}{p_a^2 p_r}+\tau=0, \frac{-\theta p}{p_b^2 p_r}+\tau=0 \\ \frac{-\omega p}{p_a p_r^2}+\frac{-\theta p}{p_b p_r^2}+\frac{\omega+\theta}{p_r^2}+\tau=0 \\ p_a+p_b+p_r-p=0\end{gathered} \tag{35}$$

After elementary manipulations, (35) can be transformed to

$$\begin{gathered}p_a=\sqrt{\varepsilon} p_b, p_r=p-p_a-p_b \\ \left(\varepsilon+1\right) p_b^2-\left(2\sqrt{\varepsilon}+2\right) p p_b+p^2=0\end{gathered} \tag{36}$$

where $\varepsilon=\omega/\theta$. By solving (36), we obtain the following two points that achieve the minimum of (33):

$$\tilde{\mathbf{p}}^1=\begin{cases}p_a=\dfrac{\varepsilon+\sqrt{\varepsilon}-\sqrt{2\varepsilon\sqrt{\varepsilon}}}{\varepsilon+1} p \\ p_b=\dfrac{\sqrt{\varepsilon}+1-\sqrt{2\sqrt{\varepsilon}}}{\varepsilon+1} p \\ p_r=\dfrac{\sqrt{2\sqrt{\varepsilon}}+\sqrt{2\varepsilon\sqrt{\varepsilon}}-2\sqrt{\varepsilon}}{\varepsilon+1} p\end{cases} \quad \tilde{\mathbf{p}}^2=\begin{cases}p_a=\dfrac{\varepsilon+\sqrt{\varepsilon}+\sqrt{2\varepsilon\sqrt{\varepsilon}}}{\varepsilon+1} p \\ p_b=\dfrac{\sqrt{\varepsilon}+1+\sqrt{2\sqrt{\varepsilon}}}{\varepsilon+1} p \\ p_r=-\dfrac{2\sqrt{\varepsilon}+\sqrt{2\varepsilon\sqrt{\varepsilon}}+\sqrt{2\sqrt{\varepsilon}}}{\varepsilon+1} p\end{cases} \tag{37}$$

Taking the inequality constraints in (32) into account, $\tilde{\mathbf{p}}^2$ should be discarded since it leads to $p_r<0$. Hence, only $\tilde{\mathbf{p}}^1$ satisfies the KKT condition and the inequality constraints in (32), which implies that $\tilde{\mathbf{p}}^1$ is the optimum solution to (32). Substituting $\tilde{\mathbf{p}}^1$ into $p_a-p_b-p_r<0$, yields $0<\varepsilon<\left(2+\sqrt{3}\right)^2$. Similarly, substituting $\tilde{\mathbf{p}}^1$ into $p_b-p_a-p_r<0$ yields $\varepsilon>\left(2-\sqrt{3}\right)^2$. Thus, $\tilde{\mathbf{p}}^1$ is valid for $\left(2-\sqrt{3}\right)^2<\varepsilon<\left(2+\sqrt{3}\right)^2$. According to the above derivations, we propose a PA strategy to minimize the outage probability and average SER, which is described as follows:

I. When $0<\varepsilon\le\left(2-\sqrt{3}\right)^2$, the power allocation is given by

$$\begin{gathered}p_a=\frac{\left[2\omega-\sqrt{2\omega^2+2\omega\theta}\right] p}{2\left(\omega-\theta\right)} \\ p_r=\frac{\left[-\left(\omega+\theta\right)+\sqrt{2\omega^2+2\omega\theta}\right] p}{2\left(\omega-\theta\right)} \\ p_b=0.5p\end{gathered} \tag{38}$$

II. When $\varepsilon \ge \left(2+\sqrt{3}\right)^2$, the power allocation is given by

$$\begin{aligned} p_a &= 0.5p \\ p_r &= \frac{\left[-(\omega+\theta)+\sqrt{2\theta^2+2\omega\theta}\right]p}{2(\theta-\omega)} \\ p_b &= \frac{\left[2\theta-\sqrt{2\theta^2+2\omega\theta}\right]p}{2(\theta-\omega)}. \end{aligned} \tag{39}$$

III. When $\left(2-\sqrt{3}\right)^2 < \varepsilon < \left(2+\sqrt{3}\right)^2$, the power allocation is given by

$$\begin{aligned} p_a &= \frac{\varepsilon+\sqrt{\varepsilon}-\sqrt{2\varepsilon\sqrt{\varepsilon}}}{\varepsilon+1}p \\ p_b &= \frac{\sqrt{\varepsilon}+1-\sqrt{2\sqrt{\varepsilon}}}{\varepsilon+1}p \\ p_r &= \frac{\sqrt{2\sqrt{\varepsilon}}+\sqrt{2\varepsilon\sqrt{\varepsilon}}-2\sqrt{\varepsilon}}{\varepsilon+1}p \end{aligned} \tag{40}$$

4.2 Optimum Relay Location under Fixed Power Allocation

In this subsection, we investigate the optimum RL with given PA to minimize the outage probability and average SER. Let the distance between T_a and T_b be so normalized that $d_a + d_b = 1$. Let $d_a = d$, and then $d_b = 1-d$. For fixed PA, the optimum RL problem can be formulated as (after substituting $\lambda = d^v$ and $\theta = (1-d)^v$ into (16))

$$\begin{aligned} d^* &= \arg\min_d Ad^v + B(1-d)^v \\ s.t.\quad & 0 < d < 1 \end{aligned} \tag{41}$$

where

$$A = \begin{cases} \dfrac{(1+J)e^{-J}}{p_r} & 1 \le \eta_1 \\ \dfrac{(1+J)e^{-J}}{\eta_1 p_r} & \eta_1 \le 1 \end{cases} \qquad B = \begin{cases} \dfrac{\eta_2}{p_r} & 1 < \eta_2 \\ \dfrac{1}{p_r} & \eta_2 \le 1. \end{cases} \tag{42}$$

The second-order derivative of $Ad^v + B(1-d)^v$ with respect of d is given by

$$v(v-1)\left[Ad^{v-2} + B(1-d)^{v-2}\right] \tag{43}$$

It is verified that (43) is positive with $d \in (0,1)$, and hence (41) is a convex optimization problem. Setting the first derivative of $Ad^v + B(1-d)^v$ with respect to d to zero, yields

$$Ad^{v-1} - B(1-d)^{v-1} = 0 \tag{44}$$

After solving (44), we obtain the optimum RL as

$$d = \left[1 + \left(\frac{A}{B} \right)^{\frac{1}{v-1}} \right]^{-1} \tag{45}$$

4.3 Joint Power Allocation and Relay Location Optimization

In this subsection, we jointly optimize the PA and RL to further minimize the outage probability and average SER. The joint optimization problem can be written as

$$\begin{aligned} (p_a, p_b, p_r, d) &= \arg \min_{p_a, p_b, p_r, d} c \\ s.t. \quad & p_a + p_b + p_r = p, \\ & p_a > 0, p_b > 0, p_r > 0, 0 < d < 1 \end{aligned} \tag{46}$$

Since finding the closed-form optimal solution to (46) is not easily tractable, we propose an iterative algorithm to effectively solve (46). The basic idea of the iterative algorithm is to alternatively optimize PA or RL with RL or PA fixed. With the results in subsection 4.1 and 4.2, the iterative optimization procedure can be summarized in **Table 1.**

Table 1 Procedure of solving problem (46)

1. Initialize p_a^0, p_b^0, p_r^0 and d^0 randomly. Calculate the cost function c^0 in (46). Set $m = 0$ and the tolarence δ.
2. Calculate the PA p_a^{m+1}, p_b^{m+1} and p_r^{m+1} with fixed d^m by using (38)-(40).
3. Calculate the RL d^{m+1} with fixed p_k^{m+1} ($k = a, b, r$) by using (45).
4. Calculate the cost function c^{m+1}. If $\left| c^{m+1} - c^m \right| < \delta$, stop iterating; otherwise, go to step 2.

Let the value of c be c_2^n (c_3^n) after calculation of step 2 (3) in the nth iteration. Since c is decreased with step 2 (3) in each iteration, we have the following sequence

$$c^0 \geq c_2^1 \geq c_3^1 \geq c_2^2 \geq c_3^2 \geq \cdots \tag{47}$$

By combing (47) and $c > 0$, it is shown through the monotonic boundary sequence theorem that the algorithm in Table 1 is convergent [33]. As verified in section 5, the joint optimization algorithm converges to a stable point within a reasonable number of iterations.

5. Simulation Results and Discussions

In this section, Monte Carlo simulation results are presented to verify the analytical results. In all simulations, we set $\gamma_{th} = 5$, $d_a + d_b = 1, v = 4$ and $\delta = 10^{-6}$. The SNR in all figures equals to total transmitting power p. The modulation type in the simulations is quadrature phase shift keying (QPSK).

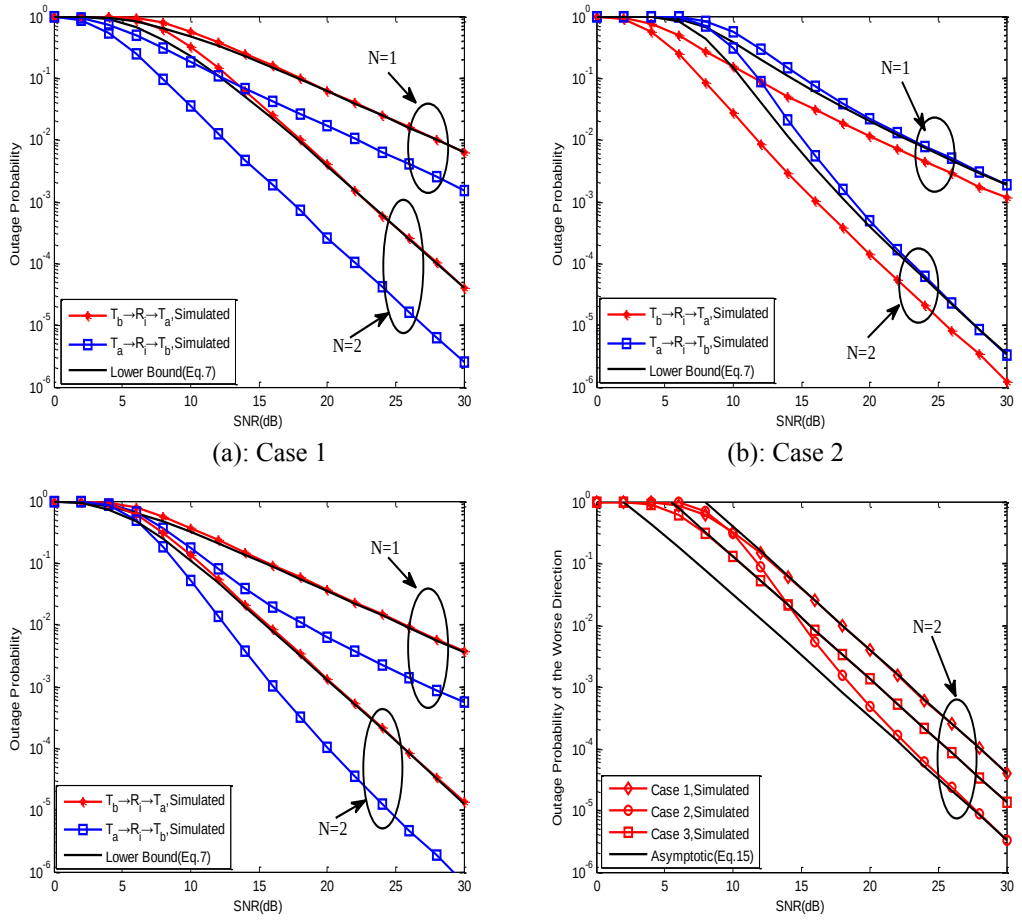

(a): Case 1 (b): Case 2

(c): Case 3 (d): $N = 2$

Fig. 2 Outage probability of the AF TWRS with max-min RS. $J = 5, d_a = d_b = 0.5$.

Case 1: $1 \le \eta_1$, $p_a = 0.6p$, $p_b = 0.2p$, $p_r = 0.2p$; Case 2: $\eta_2 \le 1$, $p_a = 0.2p$, $p_b = 0.6p$, $p_r = 0.2p$;

Case 3: $\eta_1 < 1 < \eta_2$, $p_a = 0.1p$, $p_b = 0.1p$, $p_r = 0.8p$

Fig. 2 shows the simulated, lower bound and asymptotic results of outage probability with $J = 5$ for three cases. As observed from **Fig. 2 (a)-(c)**, the numerical results of lower bound are close to the simulated results of the worse direction from medium to high SNR, which verifies the correctness of (7). Since the system works at medium or high SNR region at most times, this lower bound (7) provides guidelines for system design and optimization in practice. With further inspection on **Fig. 2 (a)-(c)**, it is shown that the lower bound excellently matches the simulated results at very low SNR (e.g., $0dB$) and high SNR (e.g., $30dB$), which can be explained as follows: i) at very low SNR, the instantaneous SNRs at the two source nodes are so small that their upper bounds obtained through (9) and $xy/(x+y) \le \min(x, y)$ are still small than the predefined threhold γ_{th}; ii) at high SNR, the approximation error in (9) is very small, and can be ignored [26]. Furthermore, $\min(x, y)$ is a quite good approximation of $xy/(x+y)$ at high SNR. For example, $\gamma_{a,i}$ can be written as $\gamma_{a,i} = e|X|^2|Y|^2 \Big/ \left[|X|^2 + |Y|^2\right]$, where $e = p_r/(p_a + p_r)$, $X = \sqrt{(p_a + p_r)}h_{a,i}$ and $Y = \sqrt{p_b}h_{b,i}$. Here, X and Y are Gaussian distributed random variables. As the SNR increases, the

variances of X and Y increase, which leads to relatively large $|X-Y|$ at most times, and implies that the approximation error can be neglected for $X \ll Y$ or $Y \ll X$. One can also observe from this **Fig.2 (d)** that the asymptotic curves are in agreement with the simulated results at high SNR, which validates the accuracy of (15). For comparison, we also plot the outage probability curves with $N=1$. It is seen that the outage probability curves have larger decreasing speed as N becomes larger, i.e., the diversity order increases with N increasing. This phenomenon demonstrates the benefits of employing multiple relays to assist transmission, and the effectiveness of max-min relay selection.

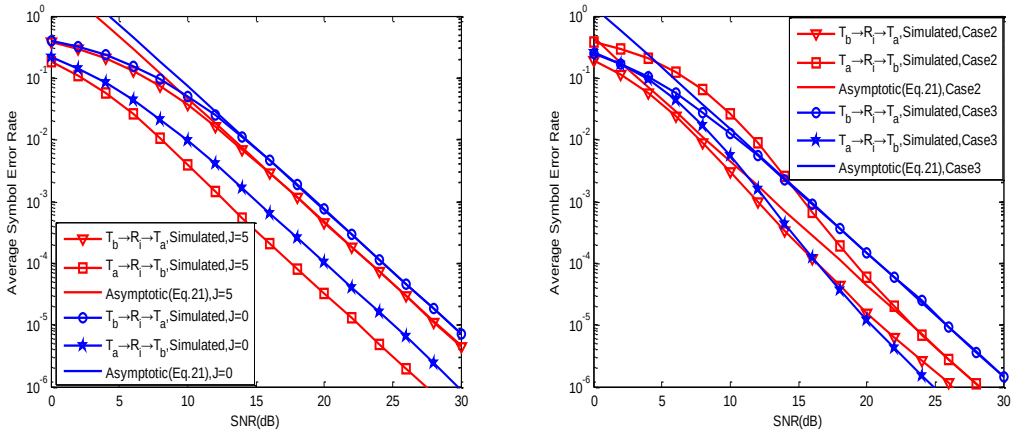

(a): Case 1, $J=0,5$ (b): Case 2 and 3, $J=5$

Fig. 3 Average SER of the TWRS with max-min RS. $N=2$, $d_a=d_b=0.5$.

Case 1: $1\le\eta_1$, $p_a=0.6p$, $p_b=0.2p$, $p_r=0.2p$;

Case 2: $\eta_2\le 1$, $p_a=0.2p$, $p_b=0.6p$, $p_r=0.2p$;

Case 3: $\eta_1<1<\eta_2$, $p_a=0.1p$, $p_b=0.1p$, $p_r=0.8p$

Fig. 3 plots the simulated and analytical results of average SER. As can clearly be seen from this figure, the asymptotic expression (21) approximates the simulated average SER of the worse direction quite well at high SNR region. It is noted from **Fig. 3 (a)** that the direction $T_b \to R_i \to T_a$ has worse performance since it has $p_b < p_a$. It is observed from **Fig. 3 (b)** that the direction $T_b \to R_i \to T_a$ still has larger average SER (Case 3), although both sources have the same transmitting power. This is due to the asymmetric fading of both hops, i.e., it has a relatively higher probability to obtain $|h_{a,i}|^2 > |h_{b,i}|^2$ with $J>0$. For comparison, the average SER curves with $J=0$ are also presented in **Fig. 3 (a)**. We can observe that the curves with $J=0$ have worse performance than those with $J=5$, which illustrates the positive impact of Rician factor. This observation also validates the analysis of Rician factor, presented in subsection 3.2.

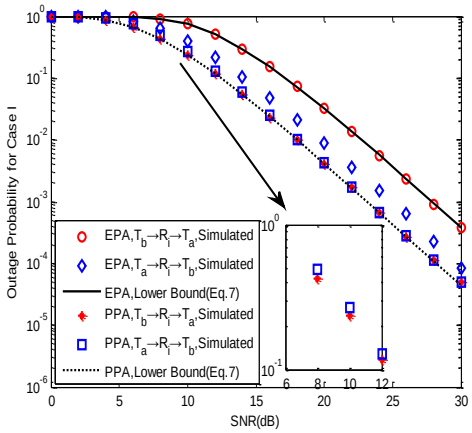

(a): Case I, outage probability

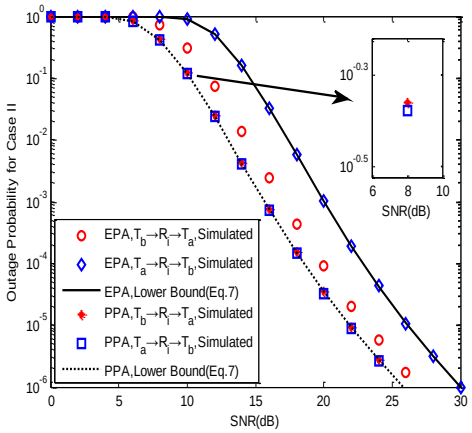

(b): Case II, outage probability

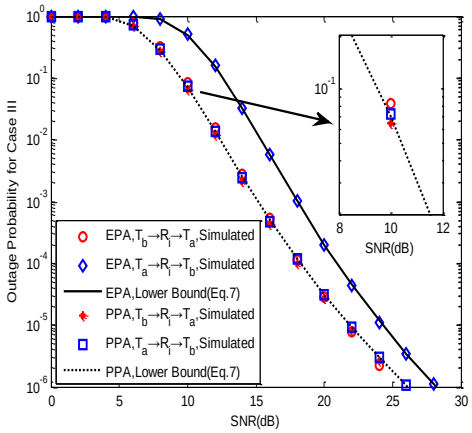

(c): Case III, outage probability

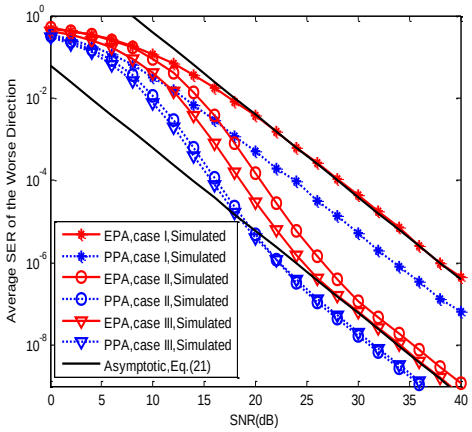

(d) Average SER

Fig. 4 Performance of the PPA and EPA schemes in the TWRS with max-min RS. $N=2, J=5$.

Case I: $\varepsilon \le \left(2-\sqrt{3}\right)^2, d_a=0.1, d_b=0.9$; Case II: $\varepsilon \ge \left(2+\sqrt{3}\right)^2, d_a=0.9, d_b=0.1$;

Case III: $\left(2-\sqrt{3}\right)^2 < \varepsilon < \left(2+\sqrt{3}\right)^2, d_a=0.8, d_b=0.2$.

Fig. 4 presents the outage probability and average SER under equal PA (EPA, $p_a=p_b=p_r=p/3$) and the proposed PA (PPA) schemes. We can see from **Fig. 4 (a)-(c)** that the lower bound excellently approximates the simulated results in the whole SNR region. This is due to the extremely asymmetric fading powers of both hops (because d_a and d_b are highly asymmetric). The values of d_a and d_b in this simulation will lead to $x>>1$ (or $y>>1$) and large $|x-y|$ at most times, and hence the lower bound based on $xy/(x+y+1) \le xy/(x+y)$ and $xy/(x+y) \le \min(x,y)$ is in excellent agreement with the simulated results in this scenario. It is obvious from **Fig. 4 (a)-(d)** that the PPA scheme outperforms the EPA scheme for three typical ε values. For example, it is seen from **Fig. 4 (a)** that about $5dB$ SNR gain is attained for case I when outage probability equals to 10^{-3}. Interestingly, we find from **Fig. 4 (a)-(c)** that the PPA scheme lead to comparable performance of the two directions $T_a \to R_i \to T_b$ and $T_b \to R_i \to T_a$. With further inspection on **Fig. 4 (a)**, it is seen that the outage probability of $T_a \to R_i \to T_b$ is slightly larger than

that of $T_b \to R_i \to T_a$ when PPA is performed, which verifies the analysis in section 4.1, i.e., the optimum value is achieved with $\eta_2 = 1(\ p_b + p_r = p_a\ )$. When $\eta_2 = 1$, the worse direction corresponds to $T_a \to R_i \to T_b$ (seen from the proof of proposition 1). It is also noted from **Fig. 4 (d)** that the performance for case I is worse than those for case II, III. This phenomenon is due to the limited channel quality of relays to T_b links. In other words, the channels between relays and T_b undergo Rayleigh fading, and the distance between relays and T_b is relatively large for case I, which leads to worse channel quality of relays to T_b links. It is also observed that the performance for case III is better than case I, II. This phenomenon indicates that the channel qualities of both hops should be balanced. Thus, ε performs as the indicator of channel balance between both hops. To get better performance, ε should not be too large or small. By further observation, it is seen that ε is relatively balanced (case III in **Fig. 4 (d)**) when the distances of both hops are not balanced ($d_a = 0.8, d_b = 0.2$). This is due to the asymmetric fading of both hops.

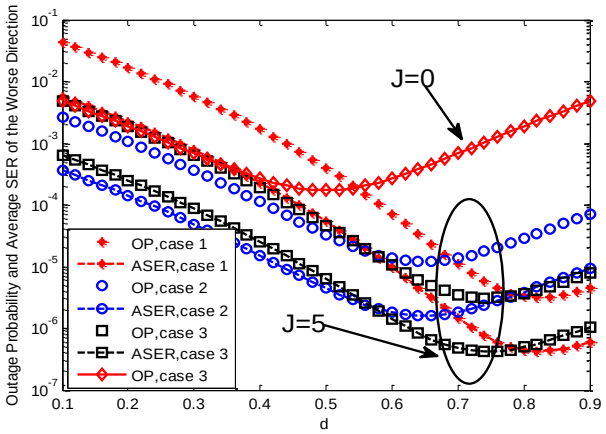

Fig. 5 Simulated outage probability and average SER of the TWRS with max-min RS.
$N = 2$, $SNR = 25dB$. Case 1: $1 \le \eta_1, p_a = 0.6p, p_b = 0.2p, p_r = 0.2p$;
Case 2: $\eta_2 \le 1, p_a = 0.2p, p_b = 0.6p, p_r = 0.2p$;
Case 3: $\eta_1 < 1 < \eta_2, p_a = 0.2p, p_b = 0.2p, p_r = 0.6p$

In **Fig. 5**, we plot the outage probability (OP) and average SER (ASER) of the worse direction as a function of d . It is seen that the optimum performances for $N = 2, J = 5$ attained at $d^* = 0.82, 0.64, 0.74$ under case 1, 2, 3, respectively, are in fine agreement with the derived result of (45). It is observed that all the optimum relay distances d for case 1, 2, 3, are larger than 0.5, which is caused by the Rician fading between relays and T_a. This demonstrates that the relays should be located near T_b to achieve channel quality balance over mixed Rician and Rayleigh fading channels. To further illustrate the benefit of channel quality balance, we also plot the outage probability curve with $J = 0$ for case 3, which attains the optimum value at $d = 0.5$. Since both T_a and T_b transmit the same power ($0.2p$) and the channels of both hops undergo Rayleigh fading ($J = 0$), the relays should be deployed at the medium location ($d = 0.5$) to achieve balance.

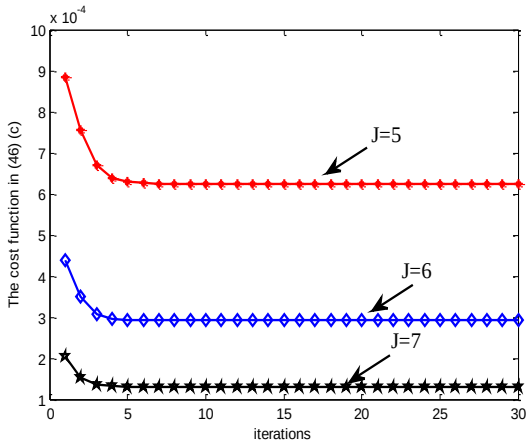

Fig. 6 Convergence behavior of the proposed iterative algorithm (**Table 1**), $SNR = 20dB$

Fig. 6 illustrates the convergence behavior of the iterative algorithm presented in **Table 1.** The curves in **Fig. 6** are obtained by initiating $p_a^0 = p_b^0 = p_r^0 = p/3$ and $d = 0.5$. It is found from this figure that the iterative algorithm converges within a reasonable number of iterations, which verifies the analysis in section 4.3.

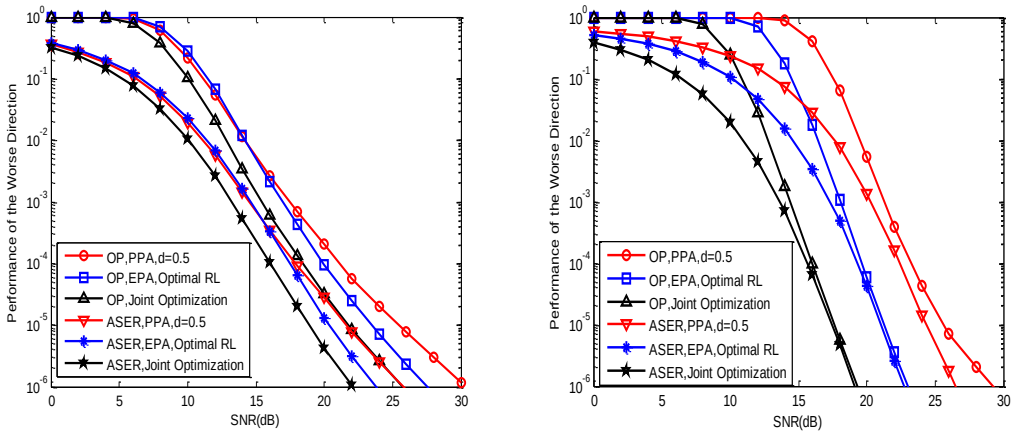

(a): $J = 5$ (b): $J = 10$

Fig. 7 Simulated performance comparison of separate PA optimization , separate RL optimization and joint PA and RL optimization

Fig. 7 shows the simulated outage probability and average SER of the worse direction with separate PA optimization, separate RL optimization and joint PA and RL optimization. It is found from **Fig. 7** that the separate RL optimization performs better than separate PA optimization, which coincides with the results in [19][20]. As expected, the joint PA and RL optimization algorithm attains larger performance gain than both separate PA and RL optimization, which verifies the effectiveness of algorithm presented in **Table 1.**

6. Conclusions

In this paper, we have investigated the AF TWRS with max-min relay selection in terms of outage probability and average SER. In particular, we considered the mixed Rician and Rayleigh fading channels, which could include the symmetric Rayleigh fading as a special case. We have derived a tight lower bound for the outage probability, which was applicable

for any transmitting powers at relays and sources. Simulation results have shown that this lower bound was quite tight at practical SNR values, which indicated that this lower bound could provide guidelines for system design in practice. The asymptotic outage probability and average SER expressions were also derived to reveal that the system with max-min relay selection could achieve full diversity order. The correctness of the asymptotic expressions has been validated by simulation results. Based on the derived expressions, we have studied the separate PA and RL optimization problems with aim to minimize both outage probability and average SER. An iterative joint PA and RL optimization algorithm was aslo proposed to further improve the system performance. We have shown through Monte Carlo simulations that the proposed separate PA scheme provided substantial performance enhancement as compared to the equal PA scheme. The effectiveness of optimal RL solution with PA fixed and joint PA and RL optimization algorithm have also been proven by simulation results.

Acknowledgements

The authors would like to appreciate the editor and the anonymous reviewers for their thorough review and insightful comments. Their sugesstions have led to significant improvement of this paper. The authors also would like to thank Prof. Xiaofu Wu and Dr. Yuhua Xu for their helpful suggestions in the revision of this paper.

References

[1] B. Rankov, A. Wittneben, "Spectral efficient protocols for half-duplex fading relay channels," *IEEE Journal on Selected Areas in Communications*, vol. 25, no. 2, pp. 379–389, February, 2007. Article (CrossRef Link).

[2] Q. Li, S. Ting, A. Pandharipande, Y. Han, "Adaptive two-way relaying and outage analysis," *IEEE Transactions on Wireless Communications*, vol. 8, no. 6, pp. 3288–3299, June, 2009. Article (CrossRef Link).

[3] P. Popovski, H. Yomo, "Wireless network coding by amplify-and-forward for bi-directional traffic flows," *IEEE Communications Letters*, vol. 11, no. 1, pp. 16–18, January, 2007. Article (CrossRef Link).

[4] T. Cui, F. Gao, T. Ho, A. Nallanathan, "Distributed space-time coding for two-way wireless relay networks," *IEEE Transactions on Signal Processing*, vol. 57, no. 2, pp. 658–671, February, 2009. Article (CrossRef Link).

[5] R. H. Y. Louie, Y. Li, B. Vucetic, "Practical physical layer network coding for two-way relay channels: performance analysis and comparison," *IEEE Transactions on Wireless Communications*, vol. 9, no. 2, pp. 764–777, February, 2010. Article (CrossRef Link).

[6] K. S. Hwang, Y. C. Ko, M. S. Alouini, "Performance bounds for two-way amplify-and-forward relaying based on relay path selection," In *Proceedings of the 2009 IEEE 69th Vehicular Technology Conference*, pp. 1–5, April, 2009. Article (CrossRef Link).

[7] S. Atapattu, Y. Jing, H. Jiang, C. Tellambura, "Opportunistic relaying in two-way networks," In *Proceddings of the 2010 5th International ICST Conference on Communications and Networking in China*, pp. 1–8, August, 2010.

[8] L. Song, "Relay selection for two-way relaying with amplify-and-forward protocols," *IEEE Transactions on Vehicular Technology*, vol. 60, no. 4, pp. 1954–1959, May, 2011. Article (CrossRef Link).

[9] P. K. Upadhyay, S. Prakriya, "Performance of two-way opportunistic relaying with analog network coding over Nakagami-m fading," *IEEE Transactions on Vehicular Technology*, vol. 60, no. 4, pp.1965–1971, May, 2011. Article (CrossRef Link).

[10] C. Wang, T. C.-K. Liu, X. Dong, "Impact of channel estimation error on the performance of AF two-way relaying," *IEEE Transactions on Vehicular Technology*, vol. 61, no. 3, pp. 1197–1207, March, 2012. Article (CrossRef Link).
[11] H. X. Nguyen, H. H. Nguyen, T. Le-Gnoc, "Diversity analysis of relay selection schemes for two-way wireless relay networks," *Wireless Personal Communications*, vol. 59, no. 2, pp. 173–189, 2011. Article (CrossRef Link).
[12] H. Ding, J. Ge, D. B. D. Costa, Y. Guo, "Outage analysis for multiuser two-way relaying in mixed Rayleigh and Rician fading," *IEEE Communications Letters*, vol. 15, no. 4, pp. 410–412, April, 2011. Article (CrossRef Link).
[13] H. Suraweera, G. Karagiannidis, P. Smith, "Performance analysis of the dual-hop asymmetric fading channel," *IEEE Transactions on Wireless Communications*, vol. 8, no. 6, pp. 2783–2788, June, 2009. Article (CrossRef Link).
[14] H. A. Suraweera, R. H. Y. Louie, Y. Li, G. K. Karagiannidis, B. Vucetic , "Two hop amplify-and-forward transmission in mixed Rayleigh and Rician fading channels," *IEEE Communications Letters*, vol. 13, no. 4, pp. 227–229, April, 2009. Article (CrossRef Link).
[15] Z. Yi, M. Ju, I. M. Kim, "Outage probability and optimum power allocation for analog network coding," *IEEE Transactions on Wireless Communications*, vol. 10, no. 2, pp. 407–412, February, 2011. Article (CrossRef Link).
[16] Y. Yang, J. Ge, Y. Gao, "Power allocation for two-way opportunistic amplify-and-forward relaying over Nakagami-m channels," *IEEE Transactions on Wireless Communications*, vol. 10, no. 7, pp. 2063–2068, July, 2011. Article (CrossRef Link).
[17] K. U. Prabhat, P. Shankar, "Performance of analog network coding with asymmetric traffic requirements," *IEEE Communications Letters*, vol. 15, no. 5, pp. 647–649, June, 2011. Article (CrossRef Link).
[18] Y. Li, X. Zhang, M. Peng, W. Wang, "Power provisioning and relay positioning for two-way relay channel with analog network coding," *IEEE Signal Processing Letters*, vol. 18, no. 9, pp. 517–520, September, 2011. Article (CrossRef Link).
[19] S. S. Ikki, S. Aissa, "A study of optimization problem for amplify-and-forward relaying over Weibull fading channels with multiple antennas," *IEEE Communication Letters*, vol. 15, no. 11, pp. 1148–1151, November, 2011. Article (CrossRef Link).
[20] S. S. Ikki, S. Aissa, "Performance evaluation and optimization of dual-hop communication over Nakagami-m fading channels in the presence of co-channel interferences," *IEEE Communications Letters*, vol. 16, no. 8, pp. 1149–1152, August, 2012. Article (CrossRef Link).
[21] S. S. Ikki, "Optimisation study of power allocation and relay location for amplify-and-forward systems over Nakagami-m fading channels," *Transaction on Emerging Telecommunications Technologies*, published online, 2012. Article (CrossRef Link).
[22] S. S. Ikki, S. Aissa, "Multihop wireless relaying systems in the presence of cochannel interference: performance analysis and design optimization," *IEEE Transactions on Vehicular Technology*, vol. 61, no. 2, pp. 566–573, February, 2012. Article (CrossRef Link).
[23] X. J. Zhang, Y. Gong, "Joint power allocation and relay positioning in multi-relay cooperative systems," *IET Communications*, vol. 3, no. 10, pp. 1683–1692, 2009. Article (CrossRef Link).
[24] M. K. Simon, M. S. Alouini, *Digital communication over fading channels: a unified approach to performance analysis*, 2nd Edition, John Wiley & Sons, New York, 2005.
[25] I. S. Gradshteyn, I. M. Ryzhik, *Table of integrals, series, and products*, 7th Edition, Academic Press, New York, 2007.
[26] M. O. Hasna, M. S. Alouini, "End-to-end performance of transmission systems with relays over Rayleigh-fading channels," *IEEE Transactions on Wireless Communications*, vol. 2, no. 6, pp. 1126–1131, November, 2003. Article (CrossRef Link).
[27] P. A. Agnhel, M. Kavheh, "Exact symbol error probability of a cooperative network in a Rayleigh-fading environment," *IEEE Transactions on Wireless Communications*, vol. 3, no. 5, pp. 1416–1421, September, 2004. Article (CrossRef Link).
[28] A. A. Abu-Dayya, N. C. Beaulieu, "Switched diversity on microcellular Ricean channels," *IEEE Transactions on Vehicular Technology*, vol. 43, no. 4, pp. 970–976, November, 1994.

Article (CrossRef Link).
[29] H. A. David, *Order Statistics,* Wiley, Hoboken, 1970.
[30] R. H. Y. Louie, Y. Li, H. A. Suraweera, B. Vucetic, "Performance analysis of beamforming in two hop amplify and forward relay networks with antenna correlation," *IEEE Transactions on Wireless Communications*, vol. 8, no. 6, pp. 3132–3141, June, 2009. Article (CrossRef Link).
[31] S. Boyd, L. Vandenberghe, *Convex Optimization*, 6th Edition, Cambridge University Press, Cambridge, 2008.
[32] D. G. Luenberger, Y. Ye, *Linear and nonlinear programming*, 3rd Edition, Springer, 2008.
[33] J. Bibby, "Axiomatisations of the average and a further generalization of monotonic sequences," *Glasgow Mathematical Journal*, vol. 15, no. 1, pp. 63–65, 1974. Article (CrossRef Link).

Zhangjun Fan received his B.Eng. degree in System Engineering from the Institute of Communications Engineering (ICE), PLA University of Science and Technology (PLAUST), Nanjing, China, 2007. He is currently working towards his Ph.D. degree in Communications and Information Systems in the same university. His current research interests include cooperative communications and resource allocation for OFDMA systems.

Daoxing Guo received his B.S., M.S. and Ph.D. degrees from the ICE, Nanjing, China, in 1995, 1999 and 2002, respectively, all in Communications and Information Systems. He is now a full professor at the ICE, PLAUST. His current research interests include cooperative communications, network coding and satellite communications.

Bangning Zhang received his B.S. and M.S. degrees from the ICE, Nanjing, China, in 1984 and 1987, respectively. He is a full professor and doctoral supervisor at the ICE, PLAUST. His research interests span the broad area of signal processing, cooperative communications, network coding and satellite communications.

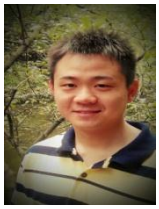

Li Zeng received his B.S. degree in Electronic Engineering from the ICE, PLAUST, 2007. He is currently working toward Ph.D. degree in signal and information processing. His research interests include compressive sensing theory, optimization theory and its application.